

A FULLY COUPLED TRANSIENT NUMERICAL MODEL OF DISK-TYPE PERMANENT MAGNET INDUCTION PUMP

*K. Paumel**, *B. Chelihhi*, *E. Sanseigne*

*CEA, DES, IRESNE, Nuclear Technology Department,
Cadarache F-13108 Saint-Paul-Lez-Durance, France*

**e-Mail: kevin.paumel@cea.fr*

This paper deals with a permanent magnet induction pump and presents a new numerical model of this pump. The fully coupled transient problem is considered. At each time step, an electromagnetic computation updates the electromagnetic force field in the fluid and feeds it to the transient fluid dynamic computation, which in turn updates the velocity field needed to update the electromagnetic computation at the next time step, and so on. The results obtained with this new model are validated by an experimental study of the recent literature and briefly compared to others numerical models of the literature. This new model has the advantage of being able to predict pressure fluctuations for fatigue analyses and minimum pressure zones for cavitation risk assessment.

Introduction.

Among different types of pumping technology used to circulate liquid metal, the permanent magnet induction pump has several advantages, especially for experimental facilities. In addition to its intrinsic tightness and high resistance to wear, like any electromagnetic pump, since it has no moving part in the liquid, its construction is very simple and cheap, while allowing a relatively high developed pressure.

Analytical models [1, 2] or semi-analytical models (e.g., using a numerical magnetostatic field simulation [3]) provide predictions of their performance, but it may be necessary to refine the modelling using numerical simulation. In particular, it is often appropriate to optimize performance (flow and developed pressure, net positive suction head required, etc.), reduce mechanical and thermal stresses, or study phenomena that may have very local origins, such as cavitation [4, 5]. Cavitation must be avoided to prevent loss of performance or damage.

The difficulty in simulating this type of electromagnetic pump is twofold. The problem is highly three dimensional, at least for disk type pumps. Indeed, the so-called drum type has been successfully represented with a 2D model [6], although Dzelme *et al.* [7] found that the 2D model overestimates the induced current density and the resulting force by neglecting the channel side effects. In addition, the frequency formulation, which simplifies the resolution of the equations, is not rigorously applicable insofar as the source of the magnetic field is discontinuous due to the magnets (unlike the harmonic excitation of coils in annular linear induction pumps, for example).

To avoid the need to consider the coupling between the fluid dynamics problem and the electromagnetic problem in full time resolution (i.e. at each time step), Koroteeva *et al.* [8] averaged the electromagnetic force over a complete revolution of the magnets and then applied it to the fluid through a steady-state RANS calculation. This approach effectively approximates the pump performance. However, it does not provide a good understanding of the flow quantities needed to assess cavitation risks or maximum stresses exerted on structures. On the other hand, Goldsteins and Buligins [9] simulated the

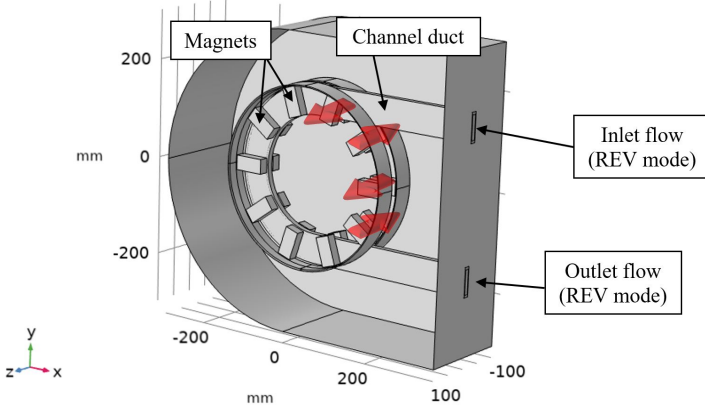


Fig. 1. 3D COMSOL[®] model showing the reference pump design. The aluminium and ferromagnetic disks are hidden in this view to let the magnets appear around the channel. For more details see [11]. The direction of magnetization is indicated by red arrows for four magnets only.

transient problem for a drum type pump, but they approximated it by considering a rectilinear geometry and a harmonic excitation. In [10], a more realistic 3D geometry was used, but the excitation field of the magnets was still modelled by a harmonic function.

In this study, the fully coupled transient problem is considered, with a representative geometry of the pump and its channel. Moreover, the magnets, with their finite excitation, are also represented. This model is applied to the pump configuration of the experiment described in [11] to compare results and to show the benefits of this new numerical scheme.

1. Reference pump design and operating conditions.

The pump design taken for reference in this study is the one manufactured at Institute for Plasma Research in India, described in detail in [11]. It consists of two magnetic disks (Fig. 1), each comprising an aluminium disk supporting ten samarium cobalt magnets, a thin ferromagnetic steel disk bound backward, and a stainless steel band ring adjusted around the disks. The gap separating the two magnetic disks is 20 mm. The pump channel, made of SS 316L, with the outer cross-section 60×12 mm and inner 50×9 mm, is placed in between. For simplicity's sake for the numerical modelling, the inlet and outlet nozzles of the channel linked to the circuit pipes have not been considered in this study. This channel contains the fluid, a heavy liquid metal alloy Pb-Li. Its temperature is maintained at 305°C . By imposing a rotational speed ν of the magnetic disks between 0 and 924 rev/min (rpm), the flowrate and developed pressure obtained by the pump varies, respectively, from 0 to a bit more than 5 l/min and from 0 to 2 bars. To study the effect of gravity, which becomes significant for such a heavy liquid, the pump was operated in both forward (FWD) and reverse (REV) mode. In [11], in the REV mode, the fluid flow follows the direction of the gravity, i.e. the inlet of the fluid is at the top and the outlet at the bottom end of the channel.

The dimensionless numbers of this problem, i.e. the Reynolds number Re , the Hartmann number Ha , the Stuart number St and the slip magnetic Reynolds number Rm_s are, respectively, defined as

$$Re = \frac{\rho_f v_f D_h}{\mu_f}, \quad Ha = B d_h \frac{\sigma_f}{\mu_f}, \quad St = \frac{B 2 \sigma_f d_h}{\rho_f v_f}, \quad Rm_s = \frac{\mu_0 \sigma_f (v_B - v_f) d_h}{\alpha d_m}, \quad (1)$$

where ρ_f , μ_f and σ_f are, respectively, the density, dynamic viscosity and electrical conductivity of the fluid. The v_f is the flow velocity and D_h is the hydraulic diameter of the channel. The v_B denotes the velocity of the magnetic field (tangential velocity of the magnets) and α the wave number: $\alpha = N_{\text{mag}}/(2R_{\text{avg}})$ with $N_{\text{mag}} = 10$ being the number of magnets in a magnetic disc, $R_{\text{avg}} = 150$ mm is the average radius of this “ring of magnets” and of the channel. The $\mu_0 = 4\pi \times 10^{-7}$ H/m stands for the magnetic permeability of vacuum. The lengths $d_h = 9$ mm and $d_m = 20$ mm represent the thickness of the fluid layer and the non-magnetic gap, respectively. Finally, $B = 0.5$ T is the magnetic field amplitude in the channel between the magnetic disks (see Fig. 2). By introducing the quantities used in the numerical model into the formula of Rm_s , it can be rewritten as

$$\text{Rm}_s = \frac{2\mu_0\sigma_f(2\pi R_{\text{avg}}\nu/60 - v_{\text{in}})d_h}{N_{\text{mag}}d_m}, \quad (2)$$

with v_{in} being the imposed uniform inlet velocity of the channel (see section 2). Hence, in this study, the Re ranges from about 6,000 to 14,000, the Ha is about 100. The N and Rms values vary from about 1 to 2 and from 0.04 to 0.22, respectively. The values of the former suggest a turbulent regime. The latter suggests that the electromagnetic quantities are only slightly affected by the flow velocity field. Finally, N of the order of unity seems to indicate that even if the magnetic field may influence the topology of turbulence, the use of a classical turbulence model (RANS, LES) remains acceptable.

2. Numerical procedure.

The problem is modelled by using the software COMSOL[®] which uses finite element modelling (FEM). For a pure CFD simulation, with a sufficiently fine mesh, which is obviously not the same for each type of modelling due to the difference in formulation and discretization, FEM and FVM (Finite Volume Modelling) will give nearly identical results. The difference will come from the computational time, which is difficult to compare due to the influence of numerous parameters: the order of the basic functions, the characteristics of the mesh, the equations to solve, etc. In this multiphysics study, the FEM has the advantage of allowing the solution of all the equations in a single scheme, facilitating the coupling between the fluid dynamics and the electromagnetics solvers.

This study is a three-dimensional temporal simulation considering a bi-directional magnetohydrodynamic coupling. At each time step, an electromagnetic computation (solving the Maxwell’s equations), performed in the overall domain, updates the electromagnetic force field in the fluid and feeds it to the transient fluid dynamics computation (solving the Navier–Stokes equations), which in turn updates the velocity field. At its turn, this new velocity field \mathbf{v} updates the electromotive force (the induced electric field) $\mathbf{E} = \mathbf{v} \times \mathbf{B}$, with \mathbf{B} being the magnetic flux density field, which in turn is used by the electromagnetic computation at the next time step, and so on.

For the fluid-dynamic problem, the RANS realizable k - ε turbulence model is preferred for its better ability to converge for this transient problem. A uniform velocity is imposed at the inlet (via the volumetric flow rate q_V), and a specified pressure (e.g., zero) is imposed at the outlet. Gravity is taken into account in the model (y -axis).

The entire pump assembly is immersed in an air volume, whose boundaries, with the inlet and the outlet of the channel, form the boundary of the whole computation domain (Fig. 1). Inside this domain, there are two other smaller air domains, each one enveloping one magnetic disk. These two domains represent the moving mesh. The channel (filled with the fluid) and the surrounding air volume form the rest of the mesh. A constant value for the rotational speed of the magnetic disks is imposed via the moving mesh.

Table 1. Physical properties of materials used in the numerical model.

Material	Electrical conductivity [S/m]	Density [kg/m ³]	Dynamic viscosity [Pa·s]
Pb-Li	8.81×10^5	9832	2.1×10^{-3}
SS 316L (channe land band ring)	9.04×10^5	–	–
Sm ₂ Co ₁₇	1.25×10^6	–	–
Aluminium	3.030×10^7	–	–

Due to its moving mesh, this model uses a combination of different electromagnetic formulations: the mixed \mathbf{A} - V_m formulation, with \mathbf{A} being the magnetic vector potential and V_m the magnetic scalar potential. The \mathbf{A} formulation is used to model current-carrying domains, and the V_m formulation is used to model the air gap and other non-conducting domains. The two formulations are coupled at their common interfacing boundaries.

Except the air (and soft iron for reasons of computational cost), all domains are considered electrically conducting. Table 1 lists the physical properties of the materials used in the model. Only the two ferromagnetic disks and the ten permanent magnets are magnetic materials (contrary to the other materials, whose magnetic property is defined by a relative permeability equal to unity). Their magnetic properties have been taken from the COMSOL[®] AC/DC library [12], and more precisely from the “soft iron” and “Sm₂Co₁₇ (BMGH-24)” material designation. The physical properties in the simulation are computed at a temperature of 305°C for the channel and the fluid and 20°C otherwise.

The choice of these magnetic properties is validated by the result of the magnetic flux density along the z -direction (Fig. 2) obtained in a section of the flow located in the path of the magnets. The shape and the amplitude are almost identical to those obtained experimentally in [11].

The mesh is made automatically by COMSOL[®] by using the default meshing as the elements size and shape are relevantly adapted relative to the physics involved in

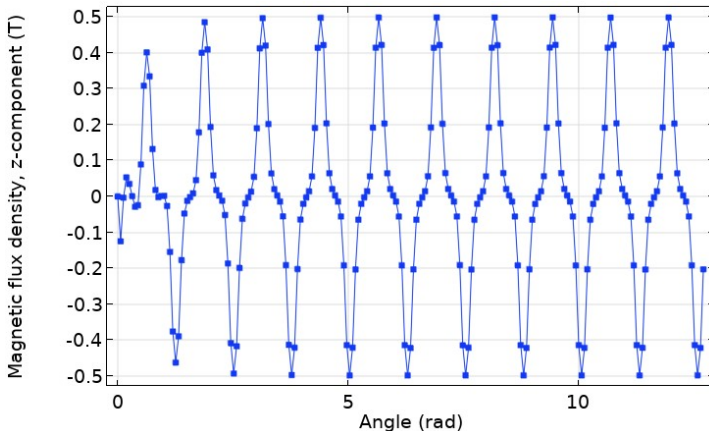


Fig. 2. Angular variation of the z -component of magnetic flux density experienced by the fluid inside the channel between the magnetic disks.

the domains. The fluid domain is the most refined domain with boundary layers meshed with prismatic elements, while the rest of the domain and all other domains are meshed with tetrahedra. Three levels of refinement have been tested: “normal” (0.12×10^6 cells), “fine” (0.38×10^6 cells) and “finer” (2.39×10^6 cells). The result difference on the developed pressure of the “normal” and “fine” versus the “finer” mesh is only 5% and 2%, respectively. All the results presented in this paper are based on the “fine” mesh.

Obviously, it is worth mentioning that this numerical procedure is also applicable to the drum-type permanent magnets pump.

3. Results.

The velocity magnitude field (Fig. 3) obtained with this new model is clearly different from Koroteeva’s [8], where waves were observed in the flow along the channel. Here the velocity profile remains quite homogenous along the “C-shape” of the channel. In the pressure field (Fig. 4), a progressive gradation is still present, but with this new model there are slight fluctuations that reflect the positions of the magnets, like a beating motion. This phenomenon is even clearer on time-lapse video of the field.

The beating behaviour also appears on the pump developed pressure versus time $\Delta p(t)$ (Fig. 5), which is the pressure difference between outlet and inlet: $\Delta p = p_{out} - p_{in}$.

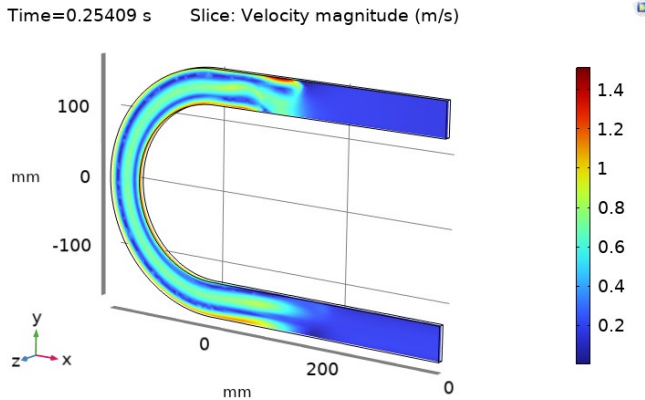


Fig. 3. Velocity magnitude field plotted on the median cut of the flow. $q_V = 3.84$ l/min and rotational speed 477 rpm in REV mode.

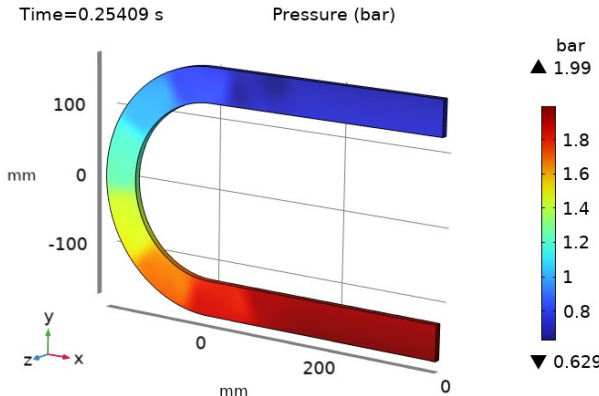


Fig. 4. Pressure field plotted in the whole fluid domain with maximum and minimum pressures of the domain indicated. $q_V = 3.84$ l/min and rotational speed 477 rpm in REV mode.

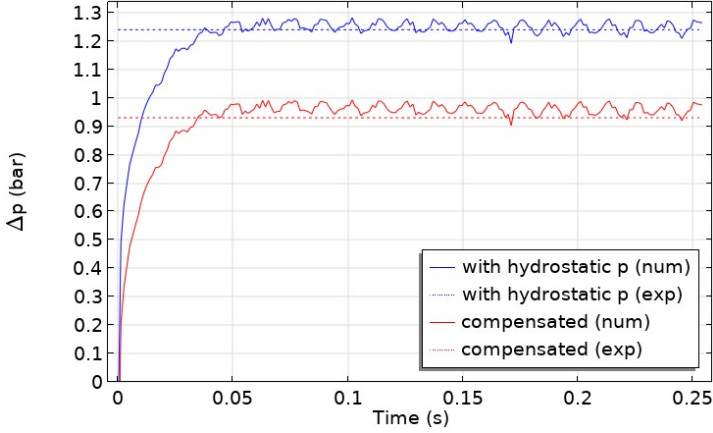


Fig. 5. Developed pressure Δp versus time of the pump without (blue) and with (red) compensation of hydrostatic pressure. Solid lines refer to numerical results and dotted lines refer to the experimental results of [6]. $q_V = 3.841/\text{min}$ and rotational speed 477 rpm in REV mode.

Table 2. Comparison between numerical and experimental developed pressures

Mode	Boundary conditions		Δp with hydrostatic pressure			Δp compensated		
	RPM	Flowrate [l/min]	Exp [bar]	Num [bar]	Diff [%]	Exp [bar]	Num [bar]	Diff [%]
REV	179	2.44	0.63	0.64	1.6	0.33	0.35	6.1
REV	328	3.20	0.94	0.94	0	0.63	0.65	3.2
REV	477	3.84	1.24	1.25	0.8	0.93	0.96	3.2
REV	626	4.38	1.54	1.56	1.3	1.22	1.27	4.1
REV	775	4.87	1.85	1.87	1.1	1.52	1.58	3.9
REV	924	5.21	2.11	2.18	3.3	1.78	1.89	6.2
FWD	477	2.42	0.51	0.70	37.3	0.78	0.99	26.9
FWD	626	2.83	0.74	1.01	36.5	1.00	1.30	30.0

This result agrees with the dynamics of the developed pressure numerically obtained in [9]. For all post-processed physical quantities, there is a transition period during which the solver converges to a stable state, due to the steep transition from initial conditions.

With numerical results, it is possible to extract the hydrostatic pressure at any point of the fluid domain. Obviously, since the fluid (Pb-Bi) is significantly heavy, the hydrostatic pressure is much greater at the bottom of the “C-shape” than near the top (0.3 bar corresponding to a pressure head of 300mm). If the latter is subtracted to the pressure at the inlet and outlet of the channel, the “compensated” (or “actual”) developed pressure of the pump can be plotted. The results of the numerical model are in very good agreement with the experimental results of Sahu [11]. The agreement is confirmed with all rotational speeds in the REV mode, as shown in Table 2.

In the FWD mode, however, the differences are significant. In this mode, at 477 rpm and beyond, the occurrence of cavitation in the experiment could explain the drop in the developed pressure relative to the predictions of the model. Indeed, Fig. 6 shows that the minimum fluid pressure in the model is nearly zero at 477 rpm (with the outlet

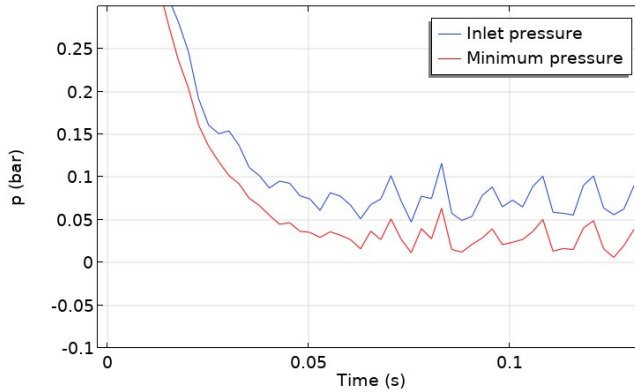


Fig. 6. Inlet and minimum pressure in FWD mode. $q_V = 2.42 \text{ l/min}$.

pressure set at 0.77 bar like in [11]), while the inlet pressure remains above 0.05 bar. At 626 rpm, the model predicts both inlet and minimum pressures less than 0 (respectively, -0.24 and -0.47 bars).

4. Conclusion.

A new numerical model of a permanent magnet induction pump has been developed with a fully coupled transient magnetohydrodynamic formulation, in which the Lorentz force is updated at each time step. It allows the representation of the fluctuating behaviour of the pressure field in a representative three dimensional geometry with magnets. This model has been validated by the Sahu's experiment with a heavy liquid metal for all rotational speeds in the REV mode. For the FWD mode, it is suggested that the differences are due to the possible occurrence of cavitation. Indeed, the minimum pressure in the fluid was very close to zero as early as 477 rpm. More generally, this numerical procedure provides a relatively detailed assessment of the Net Positive Suction Head required, NPSHr, for this type of pump (the head value at the inlet of a pump required to keep the fluid away from cavitating), especially for different liquid metal facilities operating under vacuum conditions. In addition, if a long equipment life is required, a detailed mechanical analysis, such as fatigue analysis, may be required, and again this model could provide the mechanical stresses. Finally, it should be noted that this model is capable of simulating rotational speed transient, such as a progressive increase in pump power during start-up of the equipment. On the contrary, a sudden breaking of the pump following a loss of electrical supply could be simulated to assess the stresses generated on the structures, especially the channel.

References

- [1] I. BUCENIEKS. Perspectives of using rotating permanent magnets for electromagnetic induction pump design. *Magnetohydrodynamics*, vol. 36 (2000), no. 2, pp. 151–156.
- [2] M.G. HVASTA, W.K. NOLLET, M.H. ANDERSON. Designing moving magnet pumps for high-temperature, liquid-metal systems. *Nuclear Engineering and Design*, vol. 327 (2018), pp. 228–237.

- [3] A. BREKIS *et al.* Experimental and theoretical research on disc-shaped induction-type MHD pumps with permanent magnets. *Magnetohydrodynamics*, vol. 60 (2024), no. 1-2, pp. 31–48.
- [4] K. KRAVALIS *et al.* Experimental cavitation investigation of the electromagnetic PbBi pump with rotating permanent magnets. *Magnetohydrodynamics*, vol. 58 (2022), no. 1-2, pp. 195–203.
- [5] A. BREKIS *et al.* Electromagnetic pump with rotating permanent magnets operation at low inlet pressures. *Fusion Engineering and Design*, vol. 194 (2023).
- [6] L. GOLDSTEINS. Numerical study of a centrifugal electromagnetic induction pump with zero flowrate. *Magnetohydrodynamics*, vol. 58 (2022), no. 1-2, pp. 167-176.
- [7] V. DZELME. Numerical modelling of a real rotating permanent magnet based electromagnetic induction pump. *Magnetohydrodynamics*, vol. 53 (2017), no. 4, pp. 731–737.
- [8] E. KOROTEEVA *et al.* Numerical modeling and design of a disk-type rotating permanent magnet induction pump. *Fusion Engineering and Design*, vol. 106 (2016), pp. 85–92.
- [9] L. GOLDSTEINS AND L. BULIGINS. Possibilities of 3D numerical simulations of electromagnetic induction pumps with permanent magnets. *Magnetohydrodynamics*, vol. 48 (2012), no. 4, pp. 623–635.
- [10] V. DZELME *et al.* Numerical modelling of liquid metal electromagnetic pump with rotating permanent magnets. *IOP Conf. Ser.: Mater. Sci. Eng.*, vol. 424 (2018) 012046.
- [11] SAHUS, *et al.* Effect of inlet/outlet height difference on P-Q characteristics of an electromagnetic pump for heavy liquid metals. *Fusion Engineering and Design*, vol. 197 (2023).
- [12] *AC/DC Module User's Guide, COMSOL Multiphysics®* (v. 6.1. COMSOL AB, Stockholm, Sweden, 2023).

Received 24.11.2024